

Effects of Al addition on the native defects in hafnia

Quan Li,^{a)} K. M. Koo, and W. M. Lau

Department of Physics, The Chinese University of Hong Kong, Shatin, New Territory, Hong Kong, China

P. F. Lee and J. Y. Dai

Department of Applied Physics and Materials Research Center, The Hong Kong Polytechnic University, Hung Hom, Kowloon, Hong Kong, China

Z. F. Hou and X. G. Gong^{b)}

Surface Physics Laboratory & Department of Physics, Fudan University, 200433-Shanghai, China

(Received 21 October 2005; accepted 10 March 2006; published online 3 May 2006)

Two occupied native defect bands are experimentally detected in pure HfO_2 . The density of states of band one in the middle of the band gap reduces drastically with the Al addition, while that of band two slightly above the valence-band maximum remains rather unaffected. We attribute the two bands to the charged oxygen vacancy, and the oxygen-interstitial-related defect states of the HfO_2 , respectively. We demonstrate that the added Al passivates the V_O^+ induced midgap states but has little effect on other aspects of the electronic structure of the material. © 2006 American Institute of Physics. [DOI: 10.1063/1.2196470]

The scaling requirements in the complementary metal-oxide-semiconductor (CMOS) integrated circuit technology predict the inadequacy of SiO_2 as gate dielectric material for a system smaller than $0.1 \mu\text{m}$, which leads to an extensive search of the high-dielectric constant (high- K) materials as potential replacements for SiO_2 (Ref. 1). Among these high- K dielectrics, pseudobinary Hf-based materials appear to be one of the most promising material systems and they have indeed demonstrated various desirable electrical behaviors. In such a pseudobinary system, the addition of a third element (usually Si or Al) to HfO_2 is expected to increase, relative to the properties of pure HfO_2 , the Si/dielectric interfacial stability,² crystallization temperature,³ band gap, and both the valence- and conduction-band offsets to Si (Refs. 4 and 5).

On the other hand, there are still practical deficiencies in the HfO_2 system. In particular, various native defects in HfO_2 , such as oxygen vacancy and interstitial, have been both theoretically predicted^{6,7} and experimentally observed.^{8,9} Once formed, these defects not only introduce defect levels in the band gap, but also serve as charge traps. They can thus severely affect the electrical behavior of the materials, such as leakage current and charge scattering.^{6,10} These effects become even more complicated in the pseudobinary system because the aforementioned addition of the third element in HfO_2 may interact with the native defects of HfO_2 , modify the defect states, and thereby either improve or deteriorate the electrical performance of the gate dielectrics.

To address these outstanding issues, we have carried out a systematic investigation on the electronic structure changes of a representative pseudobinary Hf-based material-hafnium aluminate as a function of aluminum concentration. In this letter, we report our experimental detection of the presence of at least two broad occupied defect bands in the band gap of the nominally pure HfO_2 films (referred to as pure HfO_2 therein), their individual changes in density of states as a function of aluminum addition, and a theoretical explanation

of these observations with *ab initio* studies.

The hafnium aluminate thin films with thickness of about 20 nm were deposited by pulsed laser deposition on *p*-type (100) Si substrates using a high-purity hafnium aluminate target with different Hf/Al ratios (Table I). The silicon substrates were treated by an HF etch just before thin-film deposition, an etch which is known to leave the silicon surface terminated by hydrogen. The X-ray photoelectron spectroscopy (XPS) measurements were carried out using a PHI Quantum 2000 system, equipped with a monochromatized Al $K\alpha$ source, a surface charge neutralizer, and a low-energy argon ion gun. All high-resolution scans were taken at a photoelectron takeoff angle of 90° and calibrated to Au $4f_{7/2}$ at 84.0 eV from a sputter-cleaned gold foil. Measurements of the Fermi-level position in the band gap were also calibrated by the threshold of photoemission of the sputter-cleaned gold reference under the same spectral resolution conditions. The microstructures of the thin films were investigated by transmission electron microscopy (TEM, Tecnai 20ST). The valence electron energy-loss measurements of the films were performed using the Gatan GIF system attached to the TEM with an energy resolution of 0.7 eV. The spectra were acquired in the diffraction mode at small momentum transfer with an angular resolution about 0.2 mrad.

The Hf/Al ratios of the films are determined from the XPS survey scan using the corresponding peak areas, as illustrated in Table I. Scanning transmission electron micros-

TABLE I. Hafnium/aluminum ratio in the hafnium aluminate target and the as-deposited thin films.

Sample	Hf/Al ratios in the targets	Hf/Al ratios in the as-deposited thin films
1	1/0	1/0
2	2/1	4/1
3	1/1	1.5/1
4	1/2	1/2
5	1/4	1/6
6	0/1	0/1

^{a)}Electronic mail: liquan@phy.cuhk.edu.hk

^{b)}Electronic mail: xggong@fudan.edu.cn

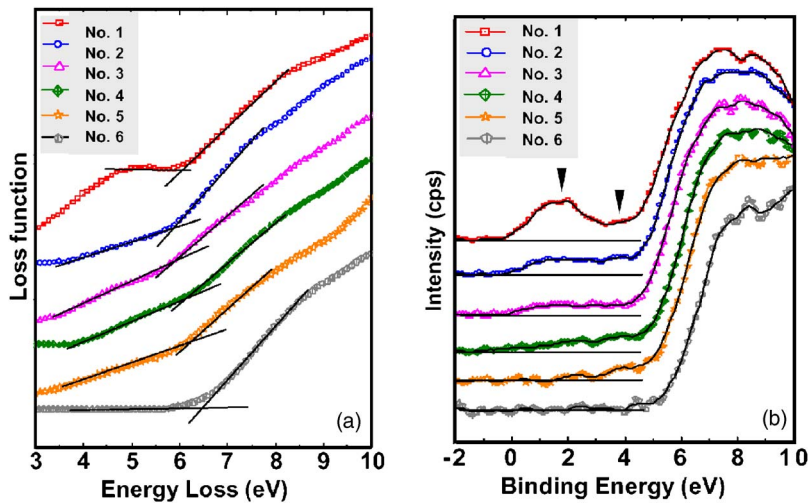


FIG. 1. (Color online) (a) Loss functions and (b) XPS low loss spectra of the Hf-Al-O thin films with different Al concentrations.

copy and transmission electron diffraction suggest similar thickness (~ 20 nm) and morphology of the all as-deposited films the films are amorphous and no interfacial layer is detected.

The loss functions ($\text{Im}-1/\epsilon$) of the films [Fig. 1(a)] are obtained by removing the plural scattering from the corresponding energy-loss spectra using a direct deconvolution method.¹¹ The band gap of pure HfO_2 is estimated to be ≈ 6.0 eV. Little change of the band gap is identified in the as-deposited films as the Al concentration increases, until pure alumina is obtained, for which the band gap is estimated as ≈ 6.5 eV, also consistent with the literature value of amorphous alumina.³ An obvious midgap band with excitation energy of 3–6 eV appears in the pure HfO_2 films. Such a feature significantly decreases when aluminum is introduced in the films, and completely diminishes in the pure alumina film.

Detailed information of the occupied midgap states above the valence-band maximum (VBM) are obtained using high-resolution XPS scan in the low-energy range (0–10 eV). The most predominant features in the spectra are the two midgap bands [centered at ≈ 2.5 eV (band I) and ≈ 0.5 eV (band II) above the VBM] observed in pure HfO_2 [as marked by arrows in Fig. 1(b)]. It is interesting to note that the two bands behave differently with the Al addition. The intensity of band I decreases drastically as the Al concentration increases in the films, and becomes undetectable when the Hf/Al ratio reaches 1/6. In comparison, little change is observed for the intensity of band II as the film composition varies, and such band only disappears in pure alumina.

From these observations, we conduct *ab initio* calculations on defects in monoclinic HfO_2 within the generalized gradient approximation (GGA) (Ref. 12), using a total-energy plane-wave pseudopotential VASP code¹³ and a supercell of 96 atoms of monoclinic HfO_2 . Atoms are removed from or added to the supercell in order to model the vacancy or interstitial defects, respectively. To simulate the Al addition, the Al substitutional defect (Al_{Hf}) is studied in the case that one of the Hf atoms in the supercell is substituted by an Al atom. The defect pairs ($\text{V}_{\text{O}}-\text{Al}_{\text{Hf}}$, $\text{O}_i-\text{Al}_{\text{Hf}}$, or $\text{O}_2-\text{Al}_{\text{Hf}}$) are formed by a substitutional Al atom and an adjacent oxygen vacancy or interstitial. The defect structures are relaxed in their various charge states until forces on all atoms were less than 0.01 eV/Å, using the ultrasoft pseudopotentials¹⁴

and a plane-wave cutoff of 500 eV. Due to the large size of the supercell, a single Γ point was employed for k -point sampling, which resulted in energy convergence of 9 meV/HfO₂. We identify the defect levels in HfO_2 by calculating the vertical ionization energies (VIP), I_p , and relaxed electron affinities (REA), χ_e , with respect to the bottom of the conduction band of HfO_2 using the equations and procedure described in Ref. 6.

The calculated ionization energies and relaxed electron affinities of these defects are summarized in Table II. Those values of the pure HfO_2 are in good agreement with the literature.⁶ The formation of a neutral oxygen vacancy introduces a fully occupied defect level with two electrons (V_{O}^0) in the middle of the band gap. The highest occupied state is located at 2.02 eV above the VBM as indicated by our calculated ionization potential (Table II).

The addition of neutral oxygen interstitials (O_i^0 and O_2^0) has two effects in general. First, the defects contribute to occupied and unoccupied defect states in the band gap. Second, they may also interact with V_{O} and thereby alter the physical properties of oxygen vacancy. Table II shows that the VIP of O_i^0 and O_2^0 are 0.04 and 0.08 eV above the VBM. Their respective REA are at 3.71 and 4.64 eV below the conduction-band minimum (CBM). Since their unoccupied states are below the highest occupied states of both V_{O} and

TABLE II. Ionization energies and electron affinities of defects in different charged states, which are corrected by the difference between the calculated band gap $E_g=3.86$ eV and experimental data $E_g^{\text{exp}}=5.68$ eV (Ref. 15).

Defects	$I_p(D^q)$		$\chi_e(D^q)$	
	This work	Ref. 6	This work	Ref. 6
V_{O}^0	3.66	3.41
V_{O}^{+}	3.48	3.75	3.01	2.76
O_i^0	5.64	5.55	3.71	3.95
O_i^{-}	5.37	5.38	5.02	4.75
O_2^0	5.60	5.53	4.64	4.67
O_2^{-}	5.42	5.46	5.13	5.06
$(\text{V}_{\text{O}}-\text{Al}_{\text{Hf}})^0$	2.97	...	2.61	...
$(\text{V}_{\text{O}}-\text{Al}_{\text{Hf}})^{+}$	5.75	...	2.33	...
$(\text{O}_i-\text{Al}_{\text{Hf}})^0$	5.62	...	5.43	...
$(\text{O}_i-\text{Al}_{\text{Hf}})^{-}$	5.61	...	1.76	...
$(\text{O}_2-\text{Al}_{\text{Hf}})^0$	5.47	...	5.07	...
$(\text{O}_2-\text{Al}_{\text{Hf}})^{-}$	5.203	...	4.50	...

V_O^+ , they can draw electrons from the oxygen vacancies and form O_i^- and O_2^- , i.e., formation of O_i (O_2) will compensate V_O , removing electrons from its defect level. The Fermi level of the system will drop accordingly. The actual behavior and electrical properties will obviously depend on the actual amounts of these defects in a real sample.

By comparing the energy levels obtained in theoretical calculation, we propose that the two defect bands observed ≈ 2.5 and ≈ 0.5 eV above the VBM in the XPS spectrum of the pure HfO_2 films can be assigned to the oxygen vacancy and interstitial related defects, respectively. These results are consistent with the relevant theoretical and experimental data in the literature.^{6,8} Due to our HfO_2 films being amorphous, the observed defect band at 2.5 eV above the VBM appears as a broad band of occupied states in our XPS spectrum, which suggests that the Fermi level of our pure HfO_2 should be at the "head" of this band near CBM, i.e., about 4 eV above the VBM. This implies that the amount of V_O must be greater than that of oxygen interstitials (O_i^0 and O_2^0). The aforementioned defect interactions among the vacancies and interstitials would therefore leave V_O^+ as a half occupied defect states with the smallest VIP in the band gap of pure HfO_2 , and thus a corresponding Fermi level in between the energy level of V_O^+ and the CBM if we also note that no interface states are observed in our HfO_2 films.

Regarding the effects of Al addition, substitution of Al at the Hf site, which is energetically favorable especially under oxygen-rich conditions, will create a hole state near the VBM because Al has three valence electrons and Hf has four. This acceptor level will compensate the V_O donor state, and remove electrons from the donor level. When Al concentration is more than twice as large as the oxygen vacancy concentration, all the electrons in the oxygen vacancy donor levels will be removed, i.e., V_O is 2+ charged. Indeed this change is demonstrated by the observed diminishing band I with Al addition in the XPS data in Fig. 1(b), although we could not exclude the possibility that the oxygen vacancy can be suppressed due to the growth condition of films in our samples from 2 to 5 (Table I). On other hand, although the Al addition also changes other occupied defect states near the VBM, the changes on their VIP are relatively small. Furthermore, Al_{Hf} itself also creates occupied defect levels near VBM contributing to the XPS signal. This explains the persistent appearance of band II in the XPS spectra of the HfO_2 films with Al addition [Fig. 1(b)]. In short, our experimental and theoretical results suggest that ionized oxygen vacancies and interstitials are the major defects observed in our experiments. This is also supported by the C - V measurement of the corresponding films after annealing at 850 °C, which sug-

gests the existence of large amounts of positively charged defects.¹⁶

In conclusion, we found that two defect bands centered at ≈ 2.5 and ≈ 0.5 eV above the VBM in pure hafnia can be identified as originating from the oxygen vacancies and oxygen interstitials, respectively. Introducing Al to the pure HfO_2 leads to interaction between Al and these defects, which passivates the occupied V_O gap states, but has little effect on other aspect of the electronic structure of the material. The current study, therefore, suggests an alternative approach to eliminate these defects, i.e., through defect engineering, by introducing an appropriate dopant to achieve the goal of gap state reduction and even elimination.

The authors are thankful for the critical comments of S.-H. Wei and D. S. Wang. X.G.G. is partially supported by the NSF of China, the national program for the basic research and research project of Shanghai. Q.L. acknowledges the RGC grant under Project No. CUHK 402105. Z.F.H. acknowledges support from Shanghai Postdoctoral Science Foundation under Grant No. 05R214106. The computation was performed at Shanghai Supercomputer Center and Supercomputer Center of Fudan.

¹G. D. Wilk, R. M. Wallace, and J. M. Anthony, *J. Appl. Phys.* **89**, 5243 (2001).

²M.-H. Cho, H. S. Chang, Y. J. Cho, D. W. Moon, K.-H. Min, R. Sinclair, S. K. Kang, D.-H. Ko, J. H. Lee, J. H. Gu, and N. I. Lee, *Appl. Phys. Lett.* **84**, 571 (2004).

³W. J. Zhu, T. Tamagawa, M. Gibson, T. Furukawa, and T. P. Ma, *IEEE Electron Device Lett.* **23**, 649 (2002).

⁴H. Y. Yu, M. F. Li, B. J. Cho, C. C. Yeo, M. S. Joo, D.-L. Kwong, J. S. Pan, C. H. Ang, J. Z. Zheng, and S. Ramanathan, *Appl. Phys. Lett.* **81**, 376 (2002).

⁵V. V. Afanas'ev, A. Stesmans, and W. Tsai, *Appl. Phys. Lett.* **82**, 245 (2003).

⁶A. S. Foster, F. Lopez, A. L. Shluger, and R. M. Nieminen, *Phys. Rev. B* **65**, 174117 (2002).

⁷K. Xiong and J. Robertson, *Microelectron. Eng.* **80**, 408 (2005).

⁸H. Takeuchi, D. Ha, and T. King, *J. Vac. Sci. Technol. A* **22**, 1337 (2004).

⁹A. Y. Kang, P. M. Lenahan, and J. F. Conley, *Appl. Phys. Lett.* **83**, 3407 (2003).

¹⁰V. V. Afanas'ev and A. Stesmans, *J. Appl. Phys.* **95**, 2518 (2004).

¹¹J. Daniels, C. von Festenberg, H. Reather, and K. Zeppenfeld, *Optical Constants of Solids by Electron Spectroscopy*, Springer Tracts in Modern Physics Vol. 54 (Springer, New York, 1970), p. 78.

¹²P. Perdew, J. A. Chevary, S. H. Vosko, K. A. Jackson, M. R. Pederson, D. J. Singh, and C. Fiolhais, *Phys. Rev. B* **46**, 6671 (1992).

¹³G. Kresse and J. Furthmüller, *Comput. Mater. Sci.* **6**, 16 (1996); G. Kresse and J. Furthmüller, *Phys. Rev. B* **54**, 11169 (1996).

¹⁴D. Vanderbilt, *Phys. Rev. B* **41**, 7892 (1990).

¹⁵M. Balog, M. Schieber, M. Michiman, and S. Patai, *Thin Solid Films* **41**, 247 (1977).

¹⁶G. D. Wilk and D. A. Muller, *Appl. Phys. Lett.* **83**, 3984 (2003).